NAVY DEPARTMENT
DAVID TAYLOR MODEL BASIN
WASHINGTON, D.C.

THE EFFECT OF AN AIR-BUBBLE SCREEN ON PRESSURES DUE TO UNDERWATER EXPLOSIONS

by

J.J. Donoghue

CONFIDENTIAL

33

August 1944

Report R-177

PERSONNEL

The tests described in this report were conducted by J.J. Donoghue, assisted by R. Baxter and F. Bird. The report was written by J.J. Donoghue with the advice and suggestions of Captain W.P. Roop, USN. Professor E.H. Kennard rendered valuable assistance with the analysis of the data.

THE EFFECT OF AN AIR-BUBBLE SCREEN ON PRESSURES DUE TO UNDERWATER EXPLOSIONS

ABSTRACT

A screen of air bubbles interposed between a small-scale underwater explosion and a pressure gage is found to cut off the pressure peak, to reduce slightly the transmitted impulse, and to reduce greatly the energy reaching the gage. Accurate observation of the later stages of the action requires the use of gage cables that do not introduce spurious signals. Attention is called to some of the nonlinear properties of bubble screens. A microflash photograph is presented, showing the progress of a shock wave along a thin sheet of air bubbles.

INTRODUCTION

An investigation of the effectiveness of a screen of air bubbles as a protection for steel structures against underwater explosions is in progress at the David Taylor Model Basin.

As a part of the investigation, the effectiveness of a thin screen of bubbles in reducing the pressure from an underwater explosion has been measured. Some preliminary results on Number 8 detonator caps and 26.5-gram charges of tetryl are presented here. The data are incomplete as the work had to be interrupted in favor of other projects of higher priority. The results so far obtained are presented in preliminary form for the information of others interested in this work.

A typical test was conducted as follows: Simultaneous measurements of the explosion pressure were first made at equal distances on opposite sides of a charge, *without* the bubble screen shown in Figure 1. These measurements were taken to check the reproducibility of the pressure records. The test was then repeated with the screen of bubbles *interposed on one side*, located midway between the charge and one pressure gage, as shown in Figure 1.

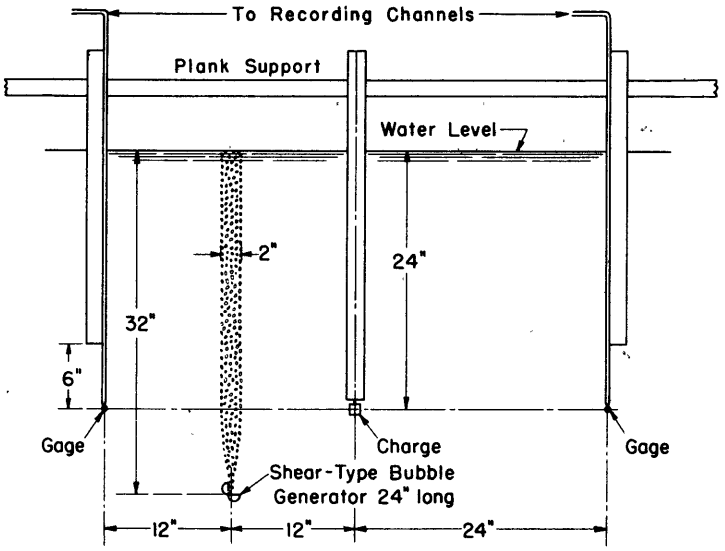

Figure 1 - Diagram of Test Arrangement for Pressure Measurements

This cross-sectional view shows the position of the charge, the pressure gages, and the bubble screen.

The bubble screen and the generator used in producing it are described in Reference (1); a photograph showing the bubble screen is shown in Figure 2.

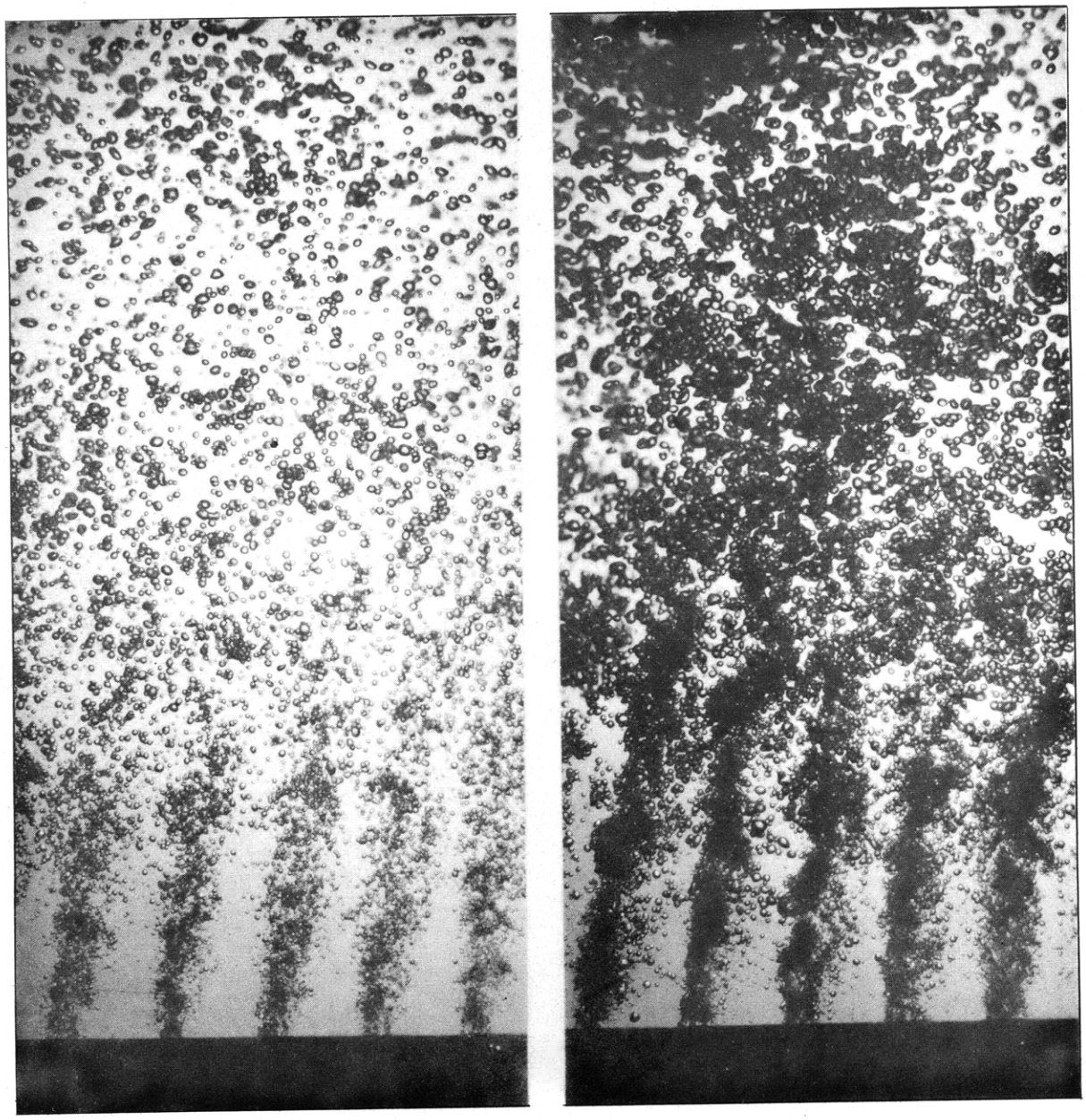

Figure 2a - The air flow is 0.017 cubic foot per minute and the water flow is 0.1 gallon per minute through each orifice. The volume concentration of air within the bubble screen is about 3 per cent.

Figure 2b - The air flow is 0.05 cubic foot per minute and the water flow is 0.1 gallon per minute through each orifice. The volume concentration of air within the bubble screen is about 9 per cent.

Figure 2 - Air-Bubble Screens Produced by the Shear-Type Bubble Generator

The depth of the actual screens is about 2 inches, measured perpendicular to the plane of the paper. The arrangement used for making these photographs is shown in Figure 3.

TEST APPARATUS

The tests were made in the high-speed basin at a point well removed from the end walls. This basin has vertical walls and a flat bottom of heavy concrete. It is 21 feet wide and the water is 10 feet deep. The pressure gages and the charge were taped to wooden sticks securely fastened to a horizontal plank supported above the water surface between two wooden platforms. The test arrangement is shown in Figure 1.

It has recently been learned, as a result of extensive tests made by the Underwater Explosives Research Laboratory at Woods Hole, that the presence of wood near gages of this kind may introduce undesirable reflections in the water. Some details of this feature of the test apparatus are discussed on page 5 in connection with the test results.

A shear-type bubble generator (1)* provided the air-bubble screen during the tests. Both air and water under pressure flow through the bubble generator.

The rate of flow of both air and water was measured with calibrated flow meters, so that the bubble screen was reproducible. The rate of flow of air was measured with a Rotameter.** The rate of flow of water was measured with a venturi-tube flow meter assembled at the Taylor Model Basin.

The distribution of the air during the tests is illustrated in Figure 2. The arrangement used to make these photographs is described below the schematic diagram in Figure 3.

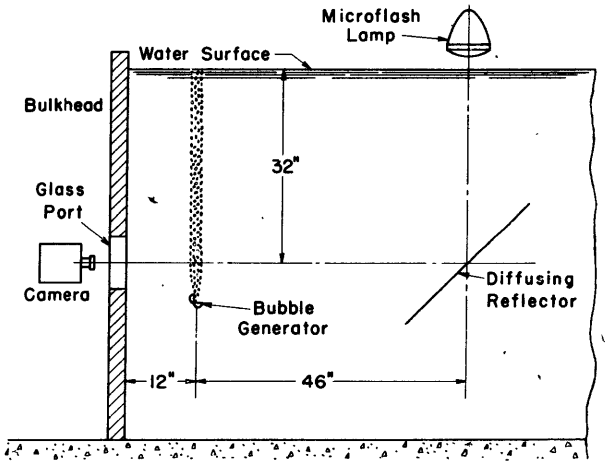

Figure 3 - Arrangement for Photographing Bubble Screens by Transmitted Light

The photographs of the bubble screen shown in Figures 2a and 2b were made with this arrangement. They were made in the small model basin, one end of which was shut off by a wooden bulkhead for the purpose. A glass port in the bulkhead permitted observation and photographic recording. Illumination of the diffusing reflector produced silhouettes of the bubbles when viewed or photographed from the glass port. The very short flash of light from the microflash lamp stopped the motion of the bubbles in the screen.

---

* Numbers in parentheses indicate references on page 23 of this report.

** This instrument is manufactured by the Fischer and Porter Company of Hatboro, Pennsylvania.

The rate of rise of these air bubbles is about 10 inches per second (2) (3). The concentration of the air was computed from this velocity, the measured rate of air flow, and the horizontal area covered by the screen.

Because the measurements were on a small scale, the thickness of the bubble screen was made as small as practicable; the thickness was approximately 1 1/2 to 2 inches. Variations in the pressure-time records may be expected if there are small variations in the bubble screen in the line between the charge and the gage at the instant the charge is detonated.

The pressures were measured with two tourmaline crystal gages supplied by Division 8 of the National Defense Research Committee (4).

The layout of a pressure-recording channel for one of the pressure gages is shown schematically in Figure 4. A single electrical impulse was initiated by the

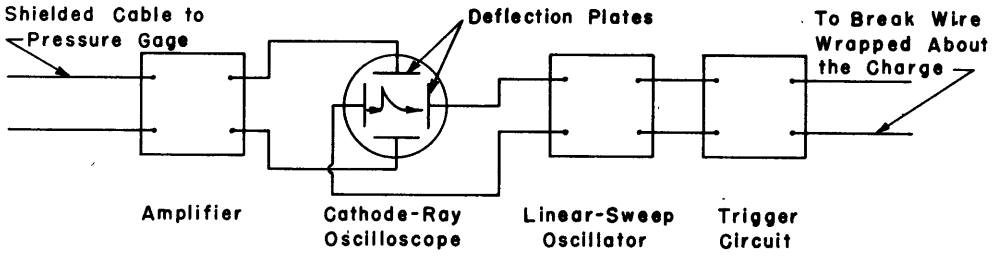

Figure 4 - A Schematic Circuit Diagram of a Pressure-Recording Channel

Each observing channel consists of a tourmaline crystal pressure gage,* a shielded cable connecting the pressure gage to the input of an amplifier, a suitable amplifier, and a cathode-ray oscilloscope; in addition, a TMB linear-sweep oscillator (5) operated by the TMB Number 8 variable time-delay trigger circuit, provides a linear time scale on the screen of the cathode-ray oscilloscope. A single sweep is initiated when the wire wrapped about the charge is broken by the explosion.

breaking of a wire wrapped about the charge. The two ends of the wire were attached to the input of the trigger circuit. The single electrical impulse appearing at the output of the trigger circuit initiated a single sweep of the sweep oscillator. The resultant motion of the fluorescent spot on the screen of the cathode-ray tube, from left to right, began just before the signal from the pressure gage appeared. The trace of the fluorescent spot was photographed with a Kodak Ektra camera.

Care was taken to remove all known sources of disturbance or distortion in the recording circuits. In particular, all the records that show the pressure transmitted by a bubble screen were made with a balanced shielded line or cable** between the pressure gage and an amplifier with a "push-pull" or balanced input. Such a cable was found to eliminate practically all the false signal generated by pressure on the underwater section of the pressure-gage cables. These cables and other details of the recording circuits are discussed in the Appendix.

* See subsequent paragraphs for a description of the gages used.

** All lines mentioned in this report were shielded microphone cables, such as Belden Numbers 8421 and 8422.

TEST RESULTS

The records taken with a wide-band or high-fidelity recording system, such as the one used for these pressure records, are characterized by an initial sharp peak, as shown in Figure 5.

The end of the wooden gage holder was 6 inches from the gage, hence the first 100 microseconds of a pressure record was assumed to be unaffected by the presence of the highly compressible wood. No effect at about this time, following the initial pressure rise, is indicated on any of the records, and it has been assumed that the presence of the wooden gage holder did not distort the form of the pressure wave.

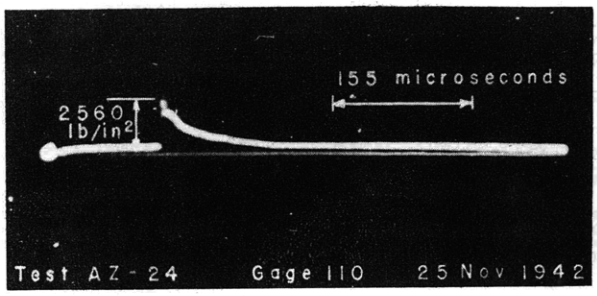

Figure 5 - Pressure-Time Record from 26.5 Grams of Tetryl at a Distance of 2 Feet

The time of rise is less than 8 microseconds. The impulse is 0.11 pound-seconds per square inch.

Since it was desired to make comparisons only of the pressures at the two locations, the calibration data supplied with the gages by the NDRC were used and the gages were not recalibrated. However, a series of observations without a bubble screen were made to obtain an idea of the consistency of the pressure data. The values of the recorded "free-field" peak pressures are listed in Table 1.

From this table it is evident that the recorded maximum pressures are not entirely uniform from one charge to the next nor do the two gages indicate the same maximum pressure. A large part of the spread is due to the poor definition of the photographic records, but asymmetry in the pressure wave about the small charge may also have caused discrepancies. The pressure gages were on opposite sides of the charge, 24 inches distant, and 24 inches below the surface, as shown in Figure 1.

Fortunately, these variations in recorded peak pressures do not affect the conclusions drawn as to the gross effects of the air-bubble screens, which greatly exceed the values of mean error shown in Table 1.

The oscillograms in Figures 6 and 7, pages 8 to 11, were chosen from the records obtained to show the effect of interposing an air-bubble screen between a charge and a pressure gage. Qualitative comparisons may be made by an inspection of pairs of oscillograms taken under the two test conditions, such as 6e and 6f, or 7b and 7c.

The bubble screen caused a delay in the arrival of the pressure at the screened gage. This is evident by comparison of two records taken at the same time under the conditions illustrated in Figure 1. For example, in Figure 6e, the time A' at which the pressure arrived at the unscreened gage was 105 microseconds after the initiation of the sweep; in Figure 6f, the time A at which the pressure arrived at the screened gage was 152 microseconds after the initiation of the sweep. The

TABLE 1

Values of Peak Pressures Recorded at a Distance of 24 Inches from the Charge

All data presented here were obtained without an air-bubble screen.

Tests whose numbers begin with AD were made with Dupont Number 8 detonator caps and those beginning with AZ with 26.5-gram charges of tetryl.

Test Number	Peak Pressure, pounds per square inch	
	Gage 106	Gage 110
AD-2*	800	650
AD-5		740
AD-8		770
AD-9		730
AD-11	800	
AD-15		760
AD-19		750
AD-21*	800	730
AD-32*	800	600
AD-33		620
AD-39*	540	530
AD-40*	650	520
AD-41	710	
AD-42	670	
AD-43	650	
AD-44	550	
Average of all records with Number 8 caps	700 ± 85 or 12.1 per cent mean error	670 ± 72 or 10.7 per cent mean error
Average of the five starred records appearing in both columns	720 ± 98 or 13.6 per cent mean error	610 ± 68 or 11.1 per cent mean error
AZ-2		3900
AZ-3		2470
AZ-4		2340
AZ-7*	3050	2900
AZ-8*	2840	3250
AZ-9	2980	
AZ-10	2850	
AZ-11	2640	
AZ-12	3000	
AZ-14		2700
AZ-15*	2660	2700
AZ-16	2700	
AZ-17	2690	
AZ-18	2800	
AZ-19	3400	
AZ-20	3210	
AZ-21	2740	
AZ-22	3200	
AZ-23	3020	
AZ-24*	2640	2560
Average of all records with 26.5-gram tetryl charges	2900 ± 194 or 6.7 per cent mean error	2852 ± 370 or 13 per cent mean error
Average of the four starred records appearing in both columns	2800 ± 148 or 5.3 per cent mean error	2852 ± 222 or 7.8 per cent mean error

same sweep generator was used for the two recording channels, so that the sweep was initiated at the same instant for both channels. Hence the delay caused by the bubble screen was 47 microseconds. The other delays shown in Figure 6 were computed in the same manner, with the aid of oscillograms not reproduced here.

The bubble screen completely stops the transmission of the incident pressure for this time interval A'A. The air bubbles collapse under the application of the pressure and thereby subtract sufficient energy from the pressure wave so that even at small concentrations of air, as indicated by Figures 6c and 6d, the incident pressure wave is stopped for a short time by the bubbles. When the wave subsequently emerges, the steep shock front has disappeared and the peak pressure is greatly reduced. The wave finally transmitted by the screen is simply the sum of the waves emitted by the collapsed bubbles themselves. The variations about a smoothly decaying pressure curve are due to phase differences between the oscillations of the various air bubbles.

Some particular features of the action of the bubble screen may be noted when the charge is 26.5 grams of tetryl. The delay A'A caused by the presence of the bubble screen is increased as the concentration of the air is increased. If the concentration of air is increased from 3 per cent as in Figure 6g, to 9 per cent as in Figure 6i, the delay is increased as much as eight times. The time of rise to the peak pressure, as indicated by the time interval AB, is also increased by the presence of the screen, but by a somewhat smaller factor than that applicable to A'A.

The later phase of the pressure is variable. The pressure drops to about 150 pounds per square inch in about 200 microseconds, and persists at about this value for as much as 250 microseconds longer. This occurs with or without the air screen, but the bubbles cause a rather violent and high-frequency fluctuation to appear, superposed on the smooth equivalent of the open-water pressure-time curve.

Figure 7 shows the effect when a Number 8 Dupont detonator is substituted for the 26.5-gram charge of tetryl.

A comparison of Figures 7a and 7c shows that the initial high-pressure peak disappears completely when the bubble screen is interposed. The peak pressure is delayed more than 150 microseconds, and reaches a value of about 67 pounds per square inch, in contrast to the "free-field" peak pressure of about 730 pounds per square inch.

Figure 7f is typical of the recorded pressure from a detonator, when a noise-free balanced line is used. The recorded pressure is believed free of cable noise, and hence the sharp peaks following the maximum pressure are probably due to bending of the tourmaline crystal, or reflections within the crystal.

The records in Figure 7 are included to show the pronounced effect of the bubble screen on the pressure from a very small charge. The nonlinear characteristics of the energy-absorbing properties of the screen are evident.

Numerical values of the impulse incident upon the gage will be found in Tables 2 and 3. These values were computed from the areas under the pressure-time

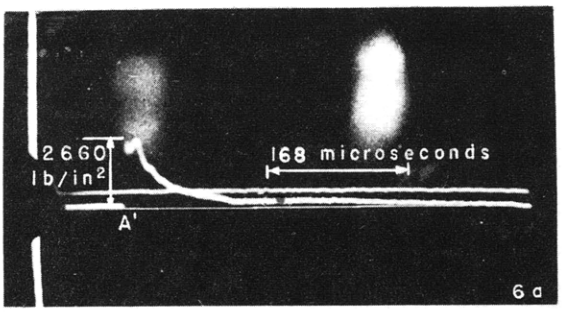

6a

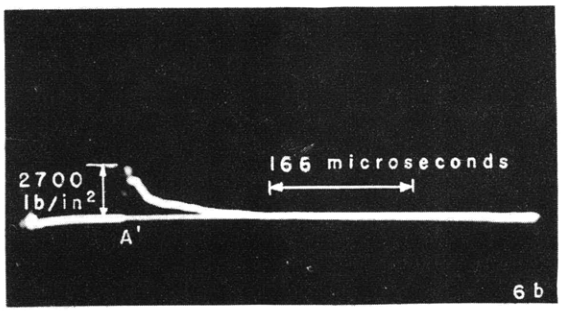

6b

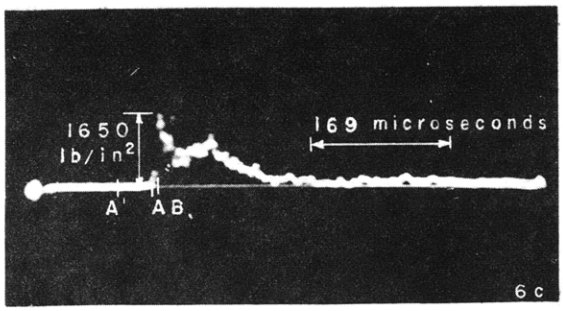

6c

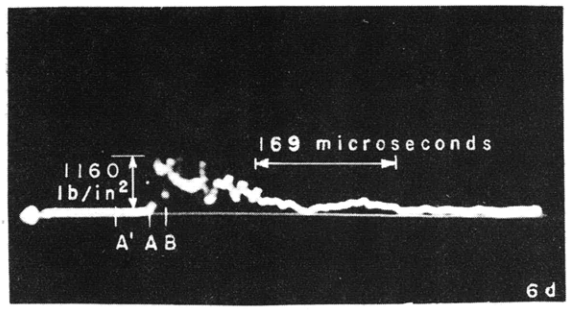

6d

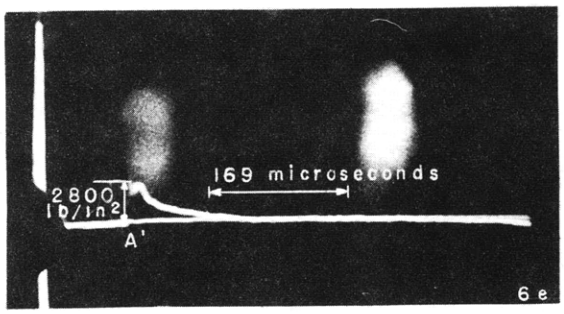

6e

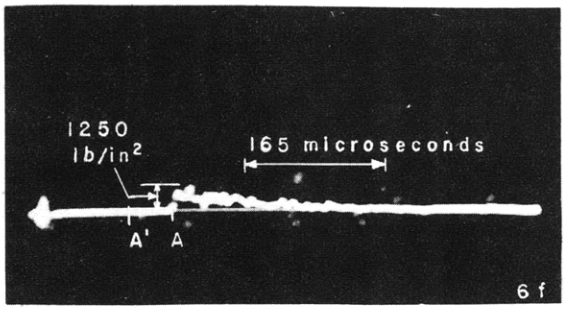

6f

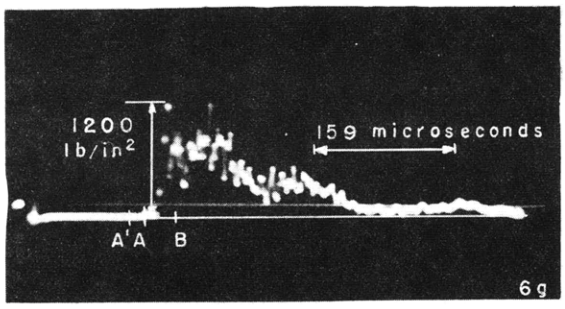

6g

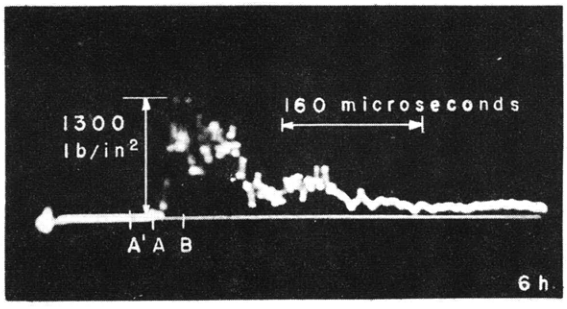

6h

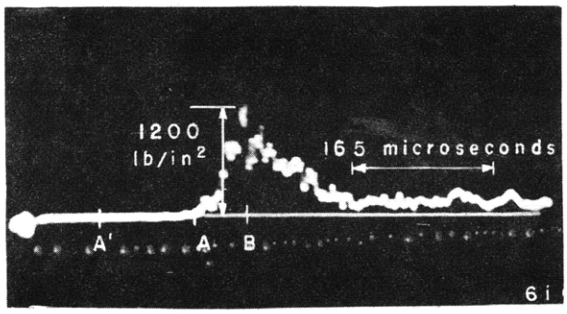

6i

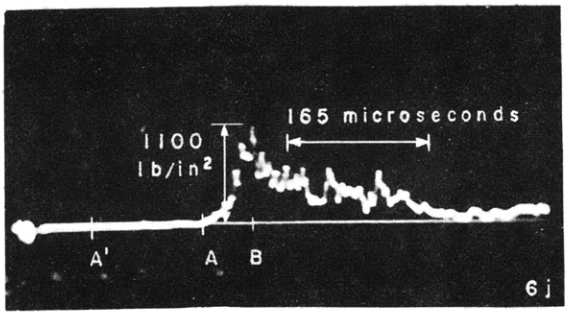

6j

Figure 6a	Test AZ-15	25 Nov 1942
Gage		106
Volume concentration of air in screen, per cent		0
Peak pressure, lb/in^2		2660
Time of rise, microseconds		< 7
Delay caused by screen, microseconds		0
Impulse, lb-sec/in^2		0.11

Figure 6b	Test AZ-15	25 Nov 1942
Gage		110
Volume concentration of air in screen, per cent		0
Peak pressure, lb/in^2		2700
Time of rise, microseconds		< 5
Delay caused by screen, microseconds		0
Impulse, lb-sec/in^2		0.11

Figure 6c	Test AZ-21	25 Nov 1942
Gage		110
Volume concentration of air in screen, per cent		2.4
Peak pressure, lb/in^2		1650
Time of rise, microseconds		10
Delay caused by screen, A'A, microseconds		47
Impulse, lb-sec/in^2		0.09

Figure 6d	Test AZ-22	25 Nov 1942
Gage		110
Volume concentration of air in screen, per cent		2.4
Peak pressure, lb/in^2		1160
Time of rise, microseconds		13
Delay caused by screen, A'A, microseconds		52
Impulse, lb-sec/in^2		0.12

Figure 6e	Test AZ-18	25 Nov 1942
Gage		106
Volume concentration of air in screen, per cent		0
Peak pressure, lb/in^2		2800
Time of rise, microseconds		< 4
Delay caused by screen, microseconds		0
Impulse, lb-sec/in^2		0.13

Figure 6f	Test AZ-18	25 Nov 1942
Gage		110
Volume concentration of air in screen, per cent		3
Peak pressure, lb/in^2		1250
Time of rise, microseconds		10
Delay caused by screen, A'A, microseconds		47
Impulse, lb-sec/in^2		0.09

Figure 6g	Test AZ-16	25 Nov 1942
Gage		110
Volume concentration of air in screen, per cent		3
Peak pressure, lb/in^2		1200
Time of rise, microseconds		15
Delay caused by screen, A'A, microseconds		15
Impulse, lb-sec/in^2		0.12

Figure 6h	Test AZ-17	25 Nov 1942
Gage		110
Volume concentration of air in screen, per cent		3
Peak pressure, lb/in^2		1300
Time of rise, microseconds		28
Delay caused by screen, A'A, microseconds		26
Impulse, lb-sec/in^2		0.14

Figure 6i	Test AZ-19	25 Nov 1942
Gage		110
Volume concentration of air in screen, per cent		9
Peak pressure, lb/in^2		1200
Time of rise, microseconds		50
Delay caused by screen, A'A, microseconds		120
Impulse, lb-sec/in^2		0.10

Figure 6j	Test AZ-20	25 Nov 1942
Gage		110
Volume concentration of air in screen, per cent		9
Peak pressure, lb/in^2		1100
Time of rise, microseconds		55
Delay caused by screen, A'A, microseconds		135
Impulse, lb-sec/in^2		0.12

Figure 6 - Pressure-Time Records from 26.5 Grams of Tetryl

For all tests, the charges were 24 inches from the gages and both the charge and the gages were at a depth of 24 inches. Refer to Figure 1 for the location of the charge, gages, and bubble screen. The screen used for Tests AZ-21 and AZ-22, Figures 6c and 6d, is not shown. Refer to Figures 2a and 2b for the size of bubbles in the screen.

The point A indicates the arrival of the shock wave at the gage when the bubble screen is in place. A'A is the delay in arrival of the shock wave caused by the presence of the bubble screen. The point A' was found by comparing each of these records with a simultaneous pressure record taken with a gage on the opposite side of the charge, as shown in Figure 1. B indicates the time at which the pressure reached the maximum. The impulse was found by integrating the pressure-time curve. A balanced or "push-pull" line was used with Gage 110 for all records.

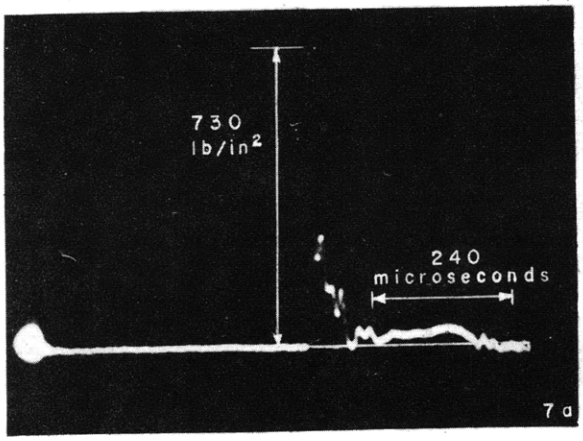
730
lb/in²
240
microseconds
7a

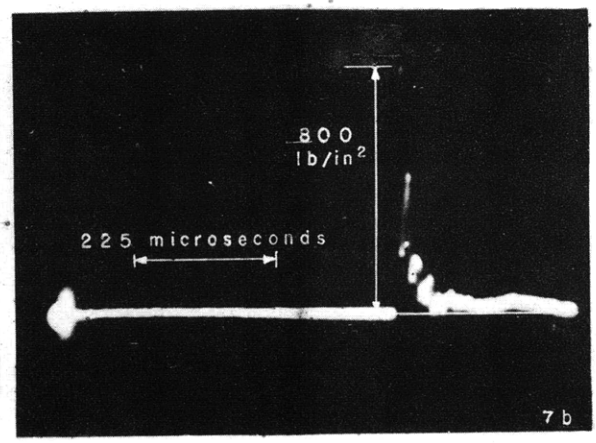
800
lb/in²
225 microseconds
7b

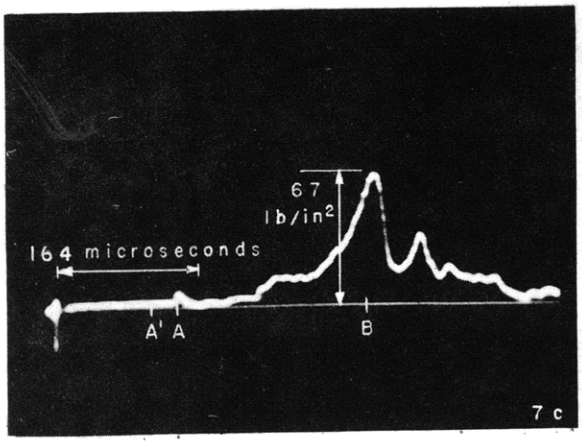
67
lb/in²
164 microseconds
A' A
B
7c

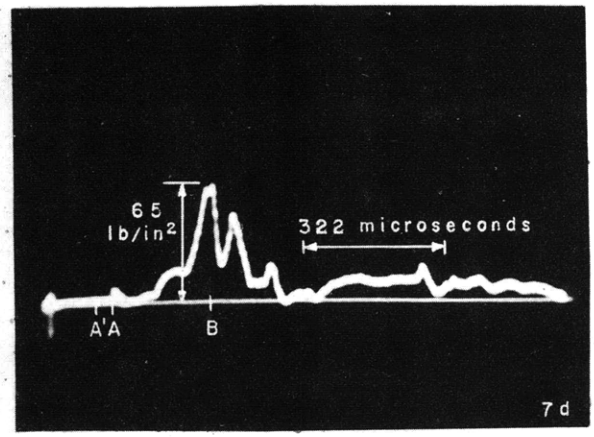
65
lb/in²
322 microseconds
A'A
B
7d

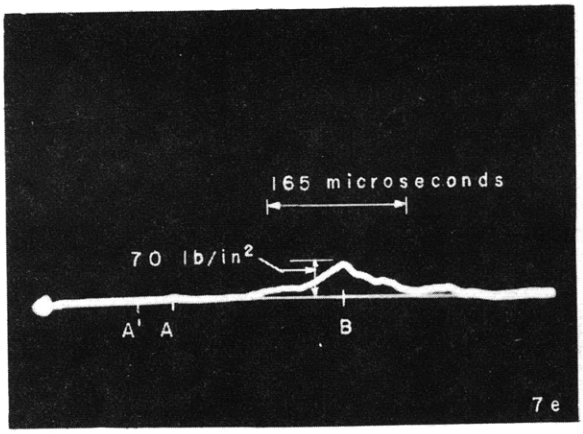
165 microseconds
70 lb/in²
A' A
B
7e

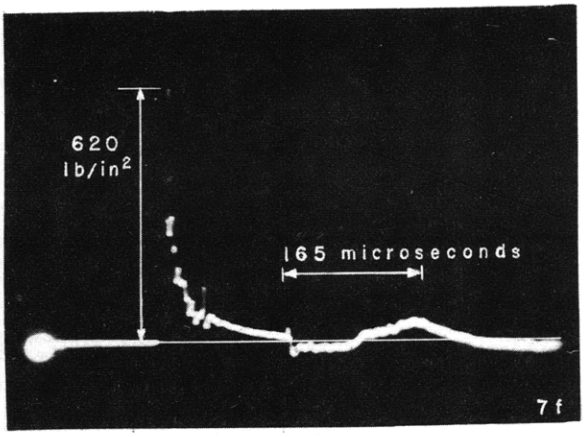
620
lb/in²
165 microseconds
7f

Figure 7a	Test AD-21	28 Oct 1942
Gage		110
Volume concentration of air in screen, per cent		0
Peak pressure, lb/in^2		730
Time of rise, microseconds		< 12
Delay caused by screen, microseconds		0
Impulse, $lb\text{-}sec/in^2$		0.018

Figure 7b	Test AD-21	28 Oct 1942
Gage		106
Volume concentration of air in screen, per cent		0
Peak pressure, lb/in^2		800
Time of rise, microseconds		< 9
Delay caused by screen, microseconds		0
Impulse, $lb\text{-}sec/in^2$		0.021

Figure 7c	Test AD-43	25 Nov 1942
Gage		110
Volume concentration of air in screen, per cent		3
Peak pressure, lb/in^2		67
Time of rise, microseconds		230
Delay caused by screen, A'A, microseconds		30
Impulse, $lb\text{-}sec/in^2$		0.007

Figure 7d	Test AD-44	25 Nov 1942
Gage		110
Volume concentration of air in screen, per cent		3
Peak pressure, lb/in^2		65
Time of rise, microseconds		220
Delay caused by screen, A'A, microseconds		50
Impulse, $lb\text{-}sec/in^2$		0.007

Figure 7e	Test AD-41	25 Nov 1942
Gage		110
Volume concentration of air in screen, per cent		3
Peak pressure, lb/in^2		70
Time of rise, microseconds		200
Delay caused by screen, A'A, microseconds		36
Impulse, $lb\text{-}sec/in^2$		0.007

Figure 7f	Test AD-33	16 Nov 1942
Gage		110
Volume concentration of air in screen, per cent		0
Peak pressure, lb/in^2		620
Time of rise, microseconds		< 7
Delay caused by screen, microseconds		0
Impulse, $lb\text{-}sec/in^2$		0.014

Figure 7 - Pressure-Time Records from a Number 8 Detonator

All conditions were identical with those described under Figure 6, except the size of the charge; also the line used with Gage 110 for the record of Figure 7a was an ordinary single-conductor microphone cable.

TABLE 2

Impulse on the Unscreened Gage

Test	See Record in Figure	Impulse, lb-sec/in^2
AZ-15	6a	0.11
AZ-15	6b	0.11
AZ-8		0.15
AZ-24	5	0.11
AZ-18	6e	0.13
AZ-22		0.16
		Average 0.13 + 0.017 (mean error)

TABLE 3

Impulse Transmitted by the Bubble Screen

Test	See Record in Figure	Impulse, lb-sec/in^2
AZ-21	6c	0.09
AZ-22	6d	0.12
AZ-23		0.09
AZ-16	6g	0.12
AZ-17	6h	0.14
AZ-18	6f	0.09
AZ-19	6i	0.10
AZ-20	6j	0.12
		Average 0.109 + 0.015 (mean error)

curves obtained with the 26.5-gram charges of tetryl. No reduction was undertaken on the data obtained with the detonator caps.

The reduction in the recorded impulse is only 16 per cent, which is near the limit of the experimental error. It may be added that there is a considerable impulse in the B-phase (6), which cannot be measured with any precision on the unscreened pressure records presented here. A study of the B-phase will be presented in a subsequent report.

ANALYSIS OF DATA AND COMPUTATIONS

It is difficult to give a quantitative discussion of the action of a thin bubble screen on a transient pressure wave of finite amplitude. The analysis given here is an over-simplified and rather qualitative discussion that ignores nonlinear

effects; it is presented in order to lead up to some of the interesting conclusions that can be drawn from the data.

The impulse in the pressure wave may be computed by the method developed in Reference (7) A pressure-time variation of the form $p = P_0 e^{-\alpha t}$ is assumed at a fixed distance from the charge; the pressure rises instantaneously to the value P_0 and falls at a rate determined by the value of α. Then the impulse in the pressure wave is given by

$$I = \int_0^\infty p\, dt = \frac{P_0}{\alpha}$$

when p is in pounds per square inch and t is in seconds.

It is known from the properties of an exponential curve that the assumed pressure falls 63 per cent in $1/\alpha$ seconds. An examination of the pressure records obtained with the unscreened gages permits an estimation of $1/\alpha$.

Using a value of $1/\alpha$ of 40×10^{-6} seconds and a value of P_0 of 2900 pounds per square inch, estimated from Figures 6a and 6b, gives

I = 0.116 pound-second per square inch at 24 inches from the charge.

This is also in rough agreement with the nominal values quoted in Reference (6).

Now consider the pressure recorded by a screened gage, as shown in Figures 6g and 6h. If pressure of the form $p = P_0 e^{-\alpha t}$ is estimated from these records, $1/\alpha$ can be approximated. By smoothing a curve through the pressure peaks, a value of 130×10^{-6} seconds is found for $1/\alpha$; P_0 is taken as 1000 pounds per square inch. The impulse I is then 0.13 pound-second per square inch; this is nearly equal to the value obtained without the screen.

However, the peak is reduced, and the decay of pressure is slowed. As a result, the corresponding energy per unit area of the wave front is radically changed. The formula for the energy in the wave is (7)

$$E = \frac{1}{2} \frac{\alpha}{\rho c} I^2$$

where ρ is the density of water in mass units per cubic inch,

c is the velocity of sound in inches per second, and

ρc = 5.3 pound-seconds per cubic inch.

At the unscreened gage the energy in the shock wave is thus found from observed data to be

E = 32 inch-pounds per square inch.

This also is in rough agreement with the nominal data of Reference (6). At the screened gage this is found to be reduced to

E = 12 inch-pounds per square inch.

The difference, 20 inch-pounds per square inch, is presumably the energy prevented by the screen from reaching the gage. The rate of fall and the peak value of the pressure have decreased, and the energy in the wave front has thus dropped about 60 per cent.

However, this diminution of energy received at the gage does not fairly represent the action at the screen, which is only half as far from the charge as the gage. In order to reduce the energy per square inch received by the gage by 20 inch-pounds per square inch it is necessary for the screen to absorb or scatter four times that much energy per square inch of screen area, or 80 inch-pounds per square inch.

No variation in transmitted energy was found at the various concentrations of air used in the tests. A comparison of Figures 6c and 6d, and 6g and 6h, with Figures 6i and 6j illustrates this. The volume concentration of air varied from 2.4 per cent for Figures 6c and 6d to 9 per cent for Figures 6i and 6j. The forms of the transmitted waves are quite similar, which indicates that the transmitted energy and impulse are little changed. Hence, it is evident that the absorption of energy has no apparent relation to the concentration of air in the bubble screen.

A measure of the maximum energy that can be absorbed by the bubble screen is given by the relation

$$E = p\Delta v$$

where p is the effective pressure and Δv is the volume occupied by the air bubbles. The expression $p\Delta v$ includes the kinetic energy given to the water surrounding the bubbles as well as the work done in compressing the gas. It is assumed that the air bubbles are compressed to negligible volume, so that Δv is the volume of air in that volume of the bubble screen included in a parallelepiped 1 inch square and of length equal to the depth of the bubble screen, i.e., 2 inches. The bubbles make up about 3 per cent of the whole volume of the screen, and Δv is thus about 0.06 cubic inch.

If the usual approximation is made that the pressure decreases as the distance from the source increases, the pressure incident on the bubble screen is $24/11 \times p_m$, where p_m is the maximum pressure observed at 24 inches from the charge in open water. By the same approximation, still assuming the source to be at a distance of 24 inches, the pressure emerging from the bubble screen is $24/13 \times p_s$, where p_s is the pressure at 24 inches from the charge when the center of the bubble screen is midway between charge and gage. From these two figures an average effective pressure on the bubbles can be deduced, and this is

$$p_a = \frac{1}{2}\left(p_s + p_m\right)$$

or

$$p_a = \frac{1}{2}\left(\frac{24}{11} \times 2900 + \frac{24}{13} \times 1000\right)$$

or

$$p_a = \frac{6350 + 1850}{2} = 4100 \text{ pounds per square inch}$$

The maximum energy that can be lost to the bubble screen is therefore

$$p_a \Delta v = 4100 \times 0.06$$

or

$$E_{max} = 246 \text{ inch-pounds per square inch}$$

The observed loss in energy, 80 inch-pounds per square inch, is less than this value and is therefore a possible value.

The observation that a change in the concentration of air in the bubble screen has no proportional effect on the pressure-time record may seem less strange after the following consideration. The velocity of transmission of the pressure front can be computed from the observed delay caused by the presence of the bubble screen. The average velocity through the bubble screen is thus found to change from about 2000 feet per second when the concentration of air is 2.4 per cent, to about 1000 feet per second when the concentration of air is 9 per cent. That the velocity should change with the concentration of air was predicted by A.B. Wood (8) among others; he assumed the air bubbles to be small compared with the wave length of the incident sound, which is also true of the tests under discussion.

Since the action of the bubble screen is to transmit the incident pressure in a distorted form after a short delay, the emitted pressure must have its source in the contractions of the individual air bubbles. It should be possible to estimate the peak pressures emitted by the individual collapsing bubbles with the aid of the theory developed in Reference (9), which indicates that the bubbles will collapse to very small diameters under a suddenly applied pressure, and will then become secondary sources of pressure.

That the bubbles do collapse to small diameters and therefore emit pressure waves of considerable amplitude is indicated also in Figure 8 in which the passage of a shock wave reveals itself to the camera. The arrangement used to make this photograph is shown in Figure 9.

From Figure 8 it is clear that the bubbles decrease in diameter rapidly when pressure is suddenly applied. Bubbles with an average diameter of about 1/8 to 3/16 inch (0.32 to 0.48 centimeter) have collapsed to about one-fifth their size in approximately 10 to 15 microseconds, following the application of the pressure whose space function is sketched upon the photograph. Their subsequent oscillation is obscured by the clouds that form about the individual bubbles.

The time of collapse may be computed with the aid of the equations developed in Reference (9). If it is assumed that a constant pressure is suddenly applied, the bubbles should collapse in a time given by Equation [19] of that reference,

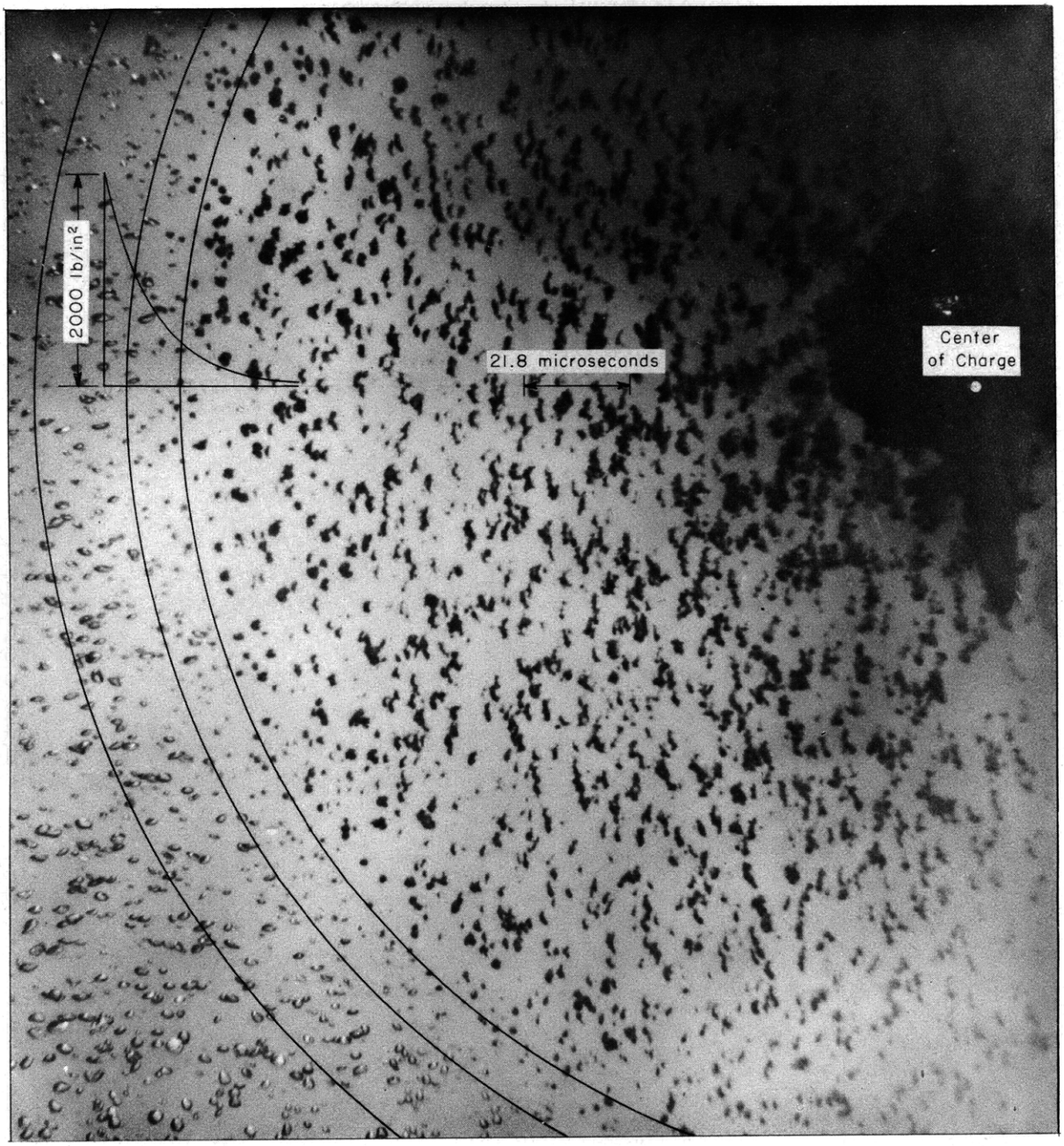

Figure 8a

This is a portion of the field in Figure 8b, reproduced to a larger scale. This microflash photograph shows the sudden collapse of small air bubbles, distributed in a vertical plane, as a shock wave passes. The concentric circles drawn in the photograph show estimated successive positions of the shock wave; the exponential curve has been placed so as to indicate about what the profile of the wave may have been at the instant of the flash.

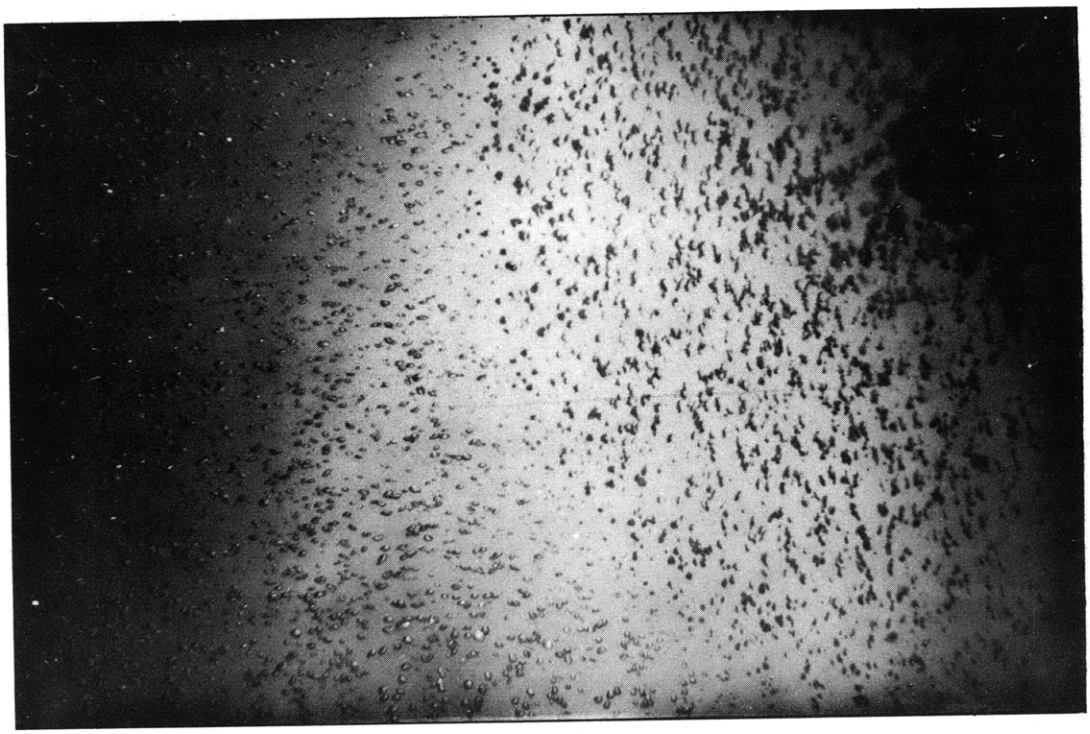

Figure 8 - The Action on a Thin Screen of Air Bubbles of the Shock Wave from a Charge Lying in the Screen

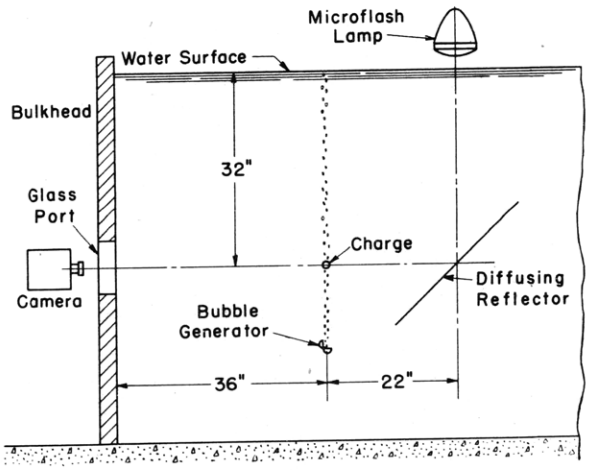

Figure 9 - Arrangement for Photographing the Passage of a Shock Wave along a Thin Screen of Air Bubbles, as Shown in Figure 8

The procedure was the same as described under Figure 3 except that the light flash was timed to follow the explosion at a predetermined interval. This was done by delaying an electrical impulse, initiated by the breaking of a wire wrapped about the charge, with the TMB Number 8 variable time-delay trigger circuit. The delayed impulse at the output of the trigger circuit set off the microflash lamp. The charge was a Number 8 detonator. The duration of the flash was 3 microseconds. The intensity of the flash was at a maximum for the middle third of the time, and rose and fell linearly. The time-delay circuit used to time the flash was not accurately reproducible; the actual position of the shock wave may be in error by 20 microseconds, which is the time required for it to travel 1.2 inch.

$$t_c = \frac{T}{2} = 0.0023 \frac{R_2}{\sqrt{p}} \text{ seconds}$$

where R_2 is the initial radius and p is the applied pressure in atmospheres. If R_2 is 1/16 inch and p is 2000 pounds per square inch or 136 atmospheres, then t_c = 12.3 microseconds.

The conditions assumed are not exactly those under which the photograph of Figure 8 was made, for in the latter case the applied pressure fell off rapidly. When the pressure drops to one atmosphere, the half-period of oscillation at large amplitudes then becomes

$$t_c = \frac{T}{2} = 144 \text{ microseconds}$$

Hence the first estimate of the time of collapse may be too small. However, a probable upper limit for the time of collapse can be set by assuming that the applied pressure is impulsive. If the initial rate of change of the radius of the bubble is computed, the time of collapse at this velocity may be estimated. This velocity is given by Equation [20] of Reference (9),

$$v_0 = -10{,}700 \frac{I}{R_2}$$

where R_2 is the initial radius of the bubble and the applied impulse is $I = P_0/\alpha$. P_0, the peak pressure, is 2000 pounds per square inch; $1/\alpha$ is very nearly 10 microseconds. Therefore

$$I = 0.02 \text{ pound-second per square inch,}$$

and the initial velocity is

$$v_0 = -3400 \text{ inches per second}$$

If this original velocity were maintained to complete collapse, the time required would be 18 microseconds for a bubble having an initial radius of 1/16 inch.

The observed time of collapse is therefore in satisfactory agreement with the theory developed in Reference (9). In that reference, there is also described the displacement of the surface of the bubble with time for various amplitudes of oscillation. The curve approximately describing the motion of a bubble under the test conditions of Figure 9 is reproduced here as Figure 10.

The observed minimum diameter in Figure 8 is about one-fifth the initial diameter, whereas the minimum diameter computed with the aid of Reference (9) is much smaller. A simple computation, however, indicates that the apparatus used to make the photograph of Figure 8 cannot be expected to reveal the true minimum diameter.

The computation requires knowledge of the minimum bubble diameter. Under a suddenly applied pressure the bubble should collapse to a diameter, $2R_1$, given by Equation [30] of Reference (9)

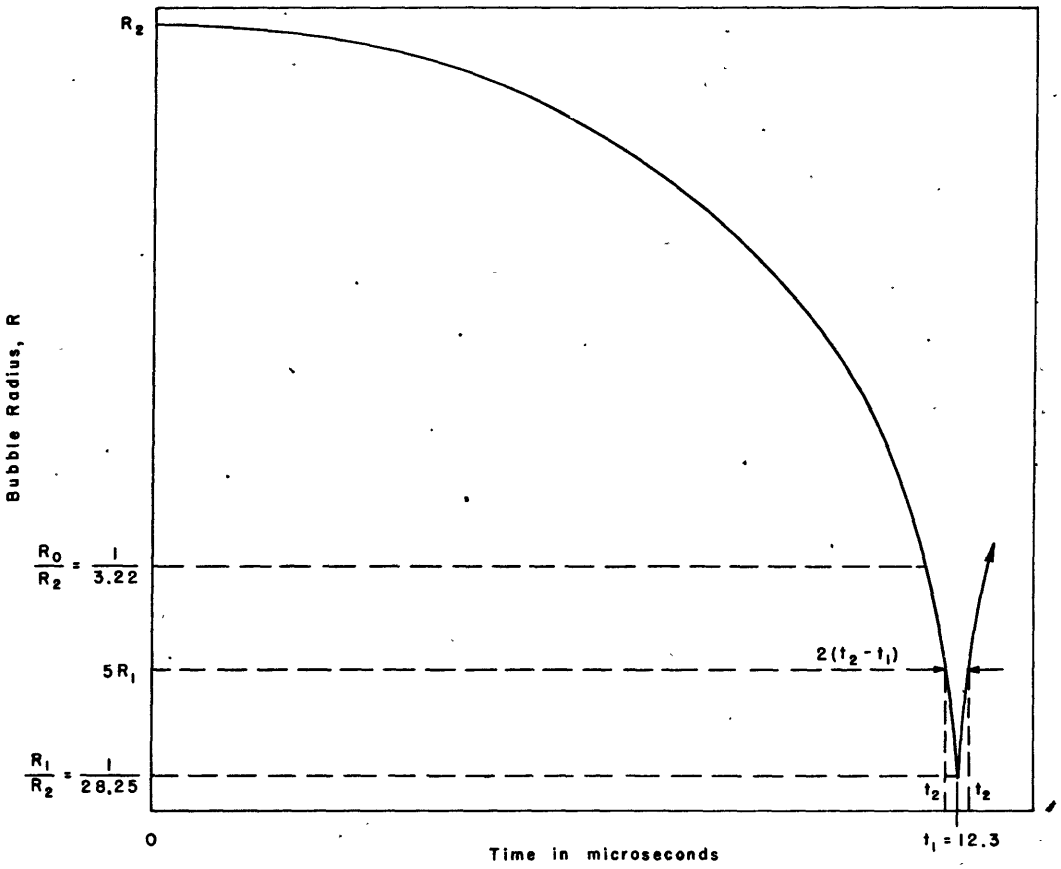

Figure 10 - Calculated Time-Displacement Curve for the Undamped Oscillation of a Bubble of Air in Water

The initial radius is 1/16 inch when a pressure P_0 = 2000 pounds per square inch is applied at $t = 0$.

t_1 = time of collapse,
R_0 = radius when in equilibrium under the applied pressure,
R_1 = minimum radius, and
R_2 = initial radius, 1/16 inch.

$$\left[\frac{R_1}{R_0}\right]^3 + \frac{1}{\gamma - 1}\left[\frac{R_0}{R_1}\right]^{3(\gamma-1)} = \left[\frac{R_2}{R_0}\right]^3 + \frac{1}{\gamma - 1}\left[\frac{R_0}{R_2}\right]^{3(\gamma-1)}$$

where γ is the ratio of the specific heats of air,

R_0 is the equilibrium radius under the new applied static pressure,

R_2 is the original radius before any pressure was applied, and

R_0 is given in terms of R_2 and the applied pressure p_0 by the adiabatic gas law

$$p_0 R_0^{3\gamma} = p_2 R_2^{3\gamma}$$

where p_2 is the original pressure.

In the present example, p_0 = 2000 pounds per square inch or 136 atmospheres, and p_2 is one atmosphere. Therefore

$$R_0 = 0.31\, R_2$$

Substituting for R_0 in the equation previously written, and putting $\gamma = 1.4$

$$\left[\frac{1}{0.31}\,\frac{R_1}{R_2}\right]^3 + 2.5\left[\frac{0.31\,R_2}{R_1}\right]^{1.2} = \left[\frac{1}{0.31}\right]^3 + 2.5\,[0.31]^{1.2}$$

The first term may be neglected in comparison with the second, since $R_1^3 << R_2^3$; therefore

$$\frac{R_2}{R_1} = 28.5$$

and

$$\frac{R_0}{R_1} = 8.8$$

The ratios of R_1 and R_0 to R_2 are indicated in Figure 10.

The minimum diameter, 1/28 the original, is much less than that observed. However, the time the bubble remains at less than, say, 5 times the minimum size is extremely small. This time may be computed with the aid of Equations [34] and [37] of Reference (9)

$$t_2 - t_1 = \frac{\sqrt{2}}{\pi}\left[2\pi R_0\sqrt{\frac{\rho}{3\,\gamma\,p_0}}\right]\left(\frac{R_1}{R_0}\right)^3\sqrt{\frac{R}{R_1} - 1}\left[\frac{8}{15} + \frac{4}{15}\,\frac{R}{R_1} + \frac{1}{5}\,\frac{R^2}{R_1^2}\right]$$

where t_1 is the time at which the bubble reaches a minimum radius R_1,
t_2 is the time at which the bubble radius is 5 R_1, and
ρ is the density of water.

At the time of minimum size, 12 microseconds after the pressure is applied, the pressure has fallen to 600 pounds per square inch. Setting p_0 = 600 pounds per square inch or 41 atmospheres, the second factor reduces to 0.00121 R_2 under the given conditions. Therefore

$$t_2 - t_1 = \frac{\sqrt{2}}{\pi}\left(0.00121\,R_2\right)\left(\frac{R_1}{R_0}\right)^3\sqrt{\frac{R}{R_1} - 1}\left[\frac{8}{15} + \frac{4}{15}\,\frac{R}{R_1} + \frac{1}{5}\,\frac{R^2}{R_1^2}\right]$$

Setting $R = 5\,R_1$ in this equation and inserting the value $R_0/R_1 = 8.78$, the time that the bubble remains below the radius $R = 5\,R_1$ is found to be

$$2(t_2 - t_1) = 3.8 \times 10^{-6} R_2 \text{ seconds}$$

When R_2 = 1/16 inch

$$2(t_2 - t_1) = 0.24 \times 10^{-6} \text{ seconds}$$

The light flash is at its peak intensity for about 1 microsecond. Since the time the bubble is at less than 5 times its minimum size is only a small part of the duration of the flash, sharp resolution of the boundary of a bubble during this phase of its oscillation is not to be expected. Throughout the duration of the peak intensity of the light flash, 1 microsecond, a bubble may collapse and return to a size 8.3 times the minimum or 0.29 times the initial size; this time interval is estimated from Figure 10. Hence an observed minimum of much less than 3 times the initial size can not reasonably be expected under these conditions. Consequently only a guess can be made as to the true minimum diameter of the bubbles. As a conservative estimate, assume that the bubbles in Tests AZ-16 and AZ-17, Figures 6g and 6h, were reduced to 1/10 their initial diameters when a peak pressure of 5800 pounds per square inch was applied. An estimate of the measured peak pressure at the pressure gage, from one collapsing bubble, may now be made. The peak pressure inside the air bubbles is

$$p_2 = p_1\left[\frac{V_1}{V_2}\right]^{\gamma} = p_1\left[\frac{r_1}{r_2}\right]^{3\gamma} = 10^{4.2} p_1 = 15{,}850\, p_1 \text{ atmospheres} = 233{,}000 \text{ lb/in}^2$$

where p_1 is the initial pressure, 1 atmosphere,
p_2 is the final pressure,
γ is the ratio of the specific heats at constant pressure and constant volume,
V_1 and V_2 are the volumes, and
r_1 and r_2 are the radii.

The pressure propagated by the bubble may now be estimated as follows: The peak pressure in a spherical compression wave is known to vary approximately inversely as the radius of the sphere. At the minimum radius of the bubble, the product of the pressure and the bubble radius is

$$p_{max} \times r_{min} = 15{,}850 \times \frac{0.0625}{10} = 99 \text{ atmosphere-inches} = k .$$

This product may now be assumed to remain constant as the distance from the source increases. Hence, at a distance of r inches, $p = k/r$, where p is the pressure at any distance r from the source.

Let r be 12 inches, the distance from the middle of the bubble screen to the pressure gage. Then p = 99/12 = 8.25 atmospheres or 120 pounds per square inch. This computed pressure is of the same order of magnitude as the observed superposed peaks of pressure found in Figure 6. Hence the assumption made as to the minimum size

reached by the bubbles appears to be a reasonable one. Likewise, the action of the bubble screen is easily explained when it is assumed that the observed pressure is the sum of the pressures propagated by the individual air bubbles.

The damping decrement of the compressed bubbles is large (10), and therefore they probably execute very few oscillations of large amplitude.

The sudden cloudiness about the air bubbles in Figure 8, after the shock wave has passed, may be caused by cavitation. The air bubbles at this point have expanded to a diameter larger than the initial one. If the expansion is great enough, the pressure in the bubbles drops below the vapor pressure of the water. Conditions are then favorable for cavitation to occur near the boundary of the bubble. The cloud thus formed would be relatively opaque to light. It is also possible that when the bubble is being compressed, air from the bubble is dissolved in the water; when it expands, the air may come out of solution and help to form a cloud about the bubble.

APPLICATIONS

The action of the bubble screen in cutting off the peak of the pressure-time curve in an underwater shock wave is associated with the absorbing, scattering, and reflecting powers of air bubbles in water, which have often been observed (8).

However, caution must be exercised before concluding that the results reported here will be duplicated under sinusoidal pressures of small amplitude. In the present instance, the bubbles extract a relatively large amount of energy from the incident wave because they undergo a large change of volume. Such large changes in volume will not occur when even the most intense underwater signaling sounds are incident on the bubbles. Hence the action of a bubble screen on pressures of small amplitudes may be quite different, particularly under steady-state conditions.

It is evident that the bubble screens described here provide a convenient way to change certain characteristics of the pressure wave. In particular, a bubble screen can be used to study the effects of a nearly constant impulse and widely different peak pressures and wave energies incident upon a test structure.

The effectiveness of bubble screens to reduce the damage to structures caused by underwater explosions will be reported in the near future.

CONCLUSIONS

When a screen of uniformly distributed small air bubbles is interposed between a small charge and a pressure gage:

a. The steep front of the pressure wave is removed or greatly decreased in amplitude.

b. The time of transmission of the pressure through the bubble screen increases as the concentration of air is increased.

c. A low pressure of relatively long duration appears in the transmitted pressure.

d. The total impulse from the pressure wave is decreased slightly.

e. The total energy in the transmitted pressure wave is sharply decreased by the presence of the bubble screen; the reduction in transmitted energy is constant over the range of concentrations of air used.

REFERENCES

(1) "Air-Bubble Generators," by J.J. Donoghue, TMB CONFIDENTIAL Report R-83, May 1943.

(2) "Rate of Rise and Diffusion of Air Bubbles in Water," by C.L. Pekeris, CONFIDENTIAL OSRD Report C4-sr20-326, October 22, 1942.

(3) "Disperse Gase III: Blasengrosze und Aufstiegzeit"(Disperse Gases III: Bubble Size and Time of Rise), by W. Luchsinger, Berlin, Kolloid-Zeitschrift, Vol. 81, No. 2, November 1937, pp. 180-182, TMB Translation 115, September 1943. Reference copy available only in TMB Library.

(4) "Measurements of Underwater Explosion Pressures," by E.B. Wilson, Jr., and R.H. Cole, OSRD Progress Report 523, 24 April 1942.

(5) "The TMB Linear Sweep Oscillator," by Ensign G. Robert Mezger, USNR, TMB Report 483, December 1941.

(6) "The Design of Ship Structure to Resist Underwater Explosion - Nominal Theory," by Captain W.P. Roop, USN, TMB CONFIDENTIAL Report 492, August 1943.

(7) "Effects of Underwater Explosions, General Considerations," by Prof. E.H. Kennard, TMB CONFIDENTIAL Report 489, September 1942.

(8) "A Textbook of Sound," by A.B. Wood, The MacMillan Company, New York, 1941, p. 362.

(9) "Radial Motion of Water Surrounding a Sphere of Gas in Relation to Pressure Waves," by Prof. E.H. Kennard, TMB CONFIDENTIAL Report 517, September 1943.

(10) "Eigenschwingung und Dämpfung von Gasblasen in Flüssigkeiten" (Natural Vibration and Damping of Gas Bubbles in Liquids), by Erwin Meyer and Konrad Tamm, Akustische Zeitschrift, Vol. 4, No. 3, May 1939. See TMB Translation 109, April 1943.

(11) "High Frequency Measurements," by August Hund, McGraw-Hill Book Company, New York, 1933, p. 112.

(12) "The Radiotron Designer's Handbook," Third Edition, edited by F. Langford Smith, RCA Manufacturing Co., Inc., Harrison, New Jersey, November 1941, p. 40, and numerous periodical references.

(13) "Relation Between Firing Current and Performance in Seismograph Caps," by L.A. Burrows, Geophysics, Vol. I, No. 2, July 1936, p. 219.

APPENDIX

DETAILS OF THE RECORDING CHANNELS

AMPLIFIERS

All amplifiers used in these pressure measurements were designed and constructed at the Taylor Model Basin to meet the requirement that when a 100-kilocycle square wave was applied to the input terminals, the output would show a time of rise of less than 1 microsecond and an overshoot of less than 3 per cent; when completed and tested, they also passed a square wave of 20 cycles per second with no measurable distortion.

Since the pressure gages used are essentially capacitive charge generators of very high resistance, the permissible change of charge in the gage circuit is strictly limited if measurable distortion is to be avoided. The presence of grid current in the input stage of the amplifier and a finite time constant of the gage circuit both introduce distortion by permitting a change in the charge generated by the gage in response to an applied pressure.

It appears of interest to examine the type of distortion to be expected from grid current in the input stage of the recording amplifier. This distortion arises as follows: The current supplied to the grid of the first tube of the amplifier through the grid resistance produces a self-bias on the tube, in addition to any fixed bias produced by other means. When a voltage is developed by the crystal pressure gage across the shunt capacitance, the voltage between grid and cathode is necessarily changed, and therefore the value of the grid current is changed. Following the change in grid current, the self-bias supplied by the grid current begins to change toward its original value; the current is supplied in part by the transfer of charge to or from the shunt capacitance forming part of the pressure-gage circuit. When the pressure is removed, the charge returned to the crystal from the shunt capacitance may be larger or smaller than that initially generated by the applied pressure and depends upon the direction of the change in the grid current. Hence, the effect is to make the duration of the recorded pressure either greater than *or* less than the true duration; the choice depends on the polarity of the applied signal. Also the return of the vacuum tube to its initial operating bias will be slow, as its rate of return is controlled by the time constant of the grid resistance and the associated capacitances which have taken on a new charge. The rectifying action of the grid may further increase the distortion of a signal of positive polarity.

One test for the presence of grid-current distortion may be made by observing the response to a square wave which has been applied to the input of the amplifier through a small coupling capacitance; this capacitance simulates the impedance of the crystal gage plus its shunt capacitance. There is another test which may be used to check any stage of the amplifier for grid-current distortion of a transmitted transient. A sine-wave signal is applied through a high impedance to the input of the

stage of the amplifier under test. The impedance is either removed or short-circuited, and in the absence of grid current, the zero-signal level as observed on the screen of a cathode-ray oscilloscope is unchanged (11).

The possibility of errors arising from excessive grid current was considered in the design of the amplifiers, and none of the amplifiers used showed measurable grid-current distortion on test.

TIME CONSTANTS AND VOLTAGE DIVIDERS

The input circuits of the amplifiers used were of two types. One was the ordinary single-side input, in which one side of the circuit is at ground potential. The other was a push-pull or balanced input. The push-pull amplifier was used with a balanced line, consisting of a cable having two conductors inside a grounded shield. The reason for using a conductor of this type is discussed in the section on "Cable Signal," page 26.

A capacitance voltage divider was needed to provide distortion-free attenuation of the signal applied to the input of the first type of amplifier. Excess gain must be available in the amplifier in order to use this type of voltage divider advantageously. The gain of the amplifier was approximately 50,000; a voltage division of 1000 to 1 or more was sometimes necessary. This type of voltage divider has the added advantage that a large time constant is provided at the input of the amplifier, so that the distortion of the later phases of the record is reduced to a negligible amount. With the circuit shown in Figure 11 the time constant RC_2 varied from 20 to 800 milliseconds.

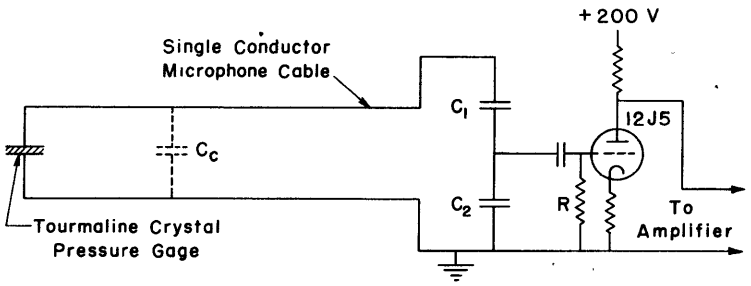

Figure 11 - Capacitance Voltage Divider Circuit

C_c is the cable capacitance, approximately 0.002 microfarad
C_1 is 0.001 microfarad
C_2 is a decade condenser, usually in 0.1-microfarad steps

The input resistance of the amplifier, R, in shunt across C_2, was 1 megohm.

The amplifier circuit as shown is schematic only.

The push-pull amplifier was equipped with an impedance-multiplying cathode follower at the input, so that the resistance presented to the gage was 10 times the grid resistance (12). The input circuit is shown schematically in Figure 12. The time constant was 24 milliseconds for all records taken with these amplifiers. A

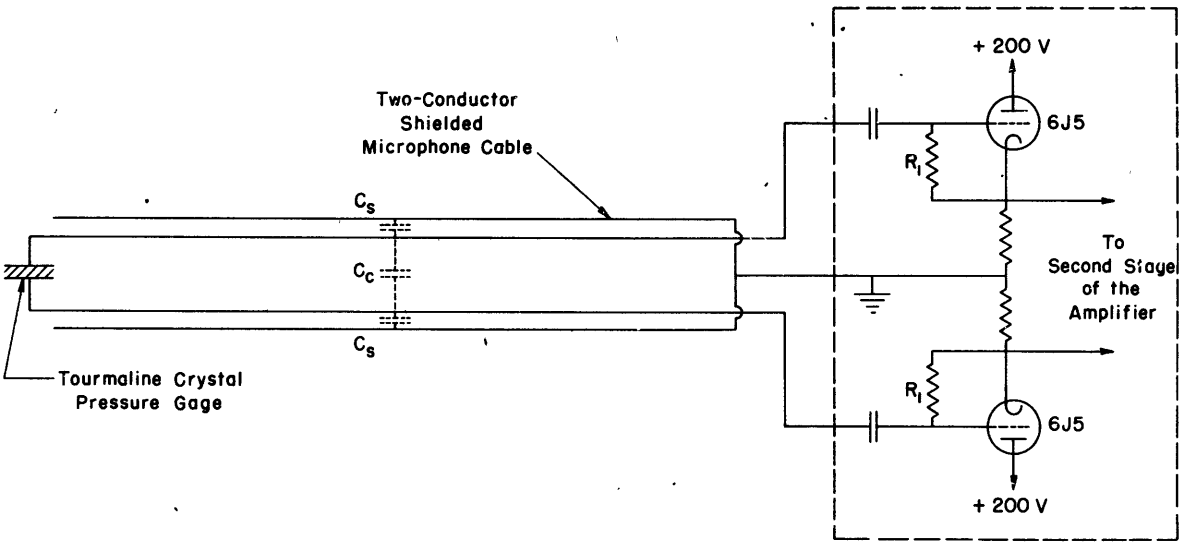

Figure 12 - Balanced Line Circuit

R_1 is 1 megohm
C_s is the capacitance between the shield and one lead
C_c is the capacitance between the leads

The effective input impedance was 20 megohms in parallel with $(C_c + C_s/2)$.
The gain of the first stage of the amplifier was 0.9.

The push-pull amplifier circuit as shown is schematic only.

step-attenuator between the first and second stages of the push-pull amplifier provided the necessary gain control. The cable from the pressure gage to the push-pull amplifier was connected directly to the amplifier. No shunt capacitance was added across the gage.

CABLES

The terminations of the cables are illustrated in Figures 11 and 12. The cables between the gages and the amplifiers were made as short as possible and the terminating capacitance was also kept small. This was done to assure low distortion arising from the improperly terminated transmission line. The lowest resonant frequency of the cables and their associated shunt capacitances was computed to be well above a megacycle in all cases.

CABLE SIGNAL

Records were taken showing the magnitude of the charge developed by various cables with no pressure gages attached, when subjected to underwater explosions identical to those described here. The results indicated that ordinary single-conductor rubber-covered microphone cable is unsuitable for crystal pressure gages when the later portion of the record, the B-phase, is to be studied. The cable signal is variable in both amplitude and duration. Its amplitude may be as much as 10 per cent of the peak signal from the gages used in the tests reported here, and it persists longer

than the pressure-gage signal.

It was found that balanced-line cables could be selected, which, when connected to a balanced push-pull amplifier, gave a cable signal less than 10 per cent of the maximum signal generated by single-conductor cables. Not all the balanced lines showed such a reduction in cable signal, but those chosen for use with these crystal gages showed consistently small signals. The charge generated by a selected cable under the above test conditions was always less than 30 micromicrocoulombs; the magnitude appeared to vary with the maximum applied pressure.

OSCILLOGRAPH WRITING SPEEDS

All peak values indicated by the arrows on the oscillograms shown in the section on "Test Results" are clearly visible on the negatives. The amplitudes had to be kept small in order to record the peak pressure at all, but many peaks were lost because of the low writing speed. The maximum writing speed is that velocity of the spot on the fluorescent screen of the cathode-ray tube that can be recorded photographically. The available writing speed was not high enough to record the initial peak pressure with certainty at amplitudes larger than those shown. At the highest recorded velocities, during the initial pressure rise, the spot did not leave a trace on the photograph.

TIME DELAY

A single sweep was used for all records. The initiation of the more rapid sweeps was timed by a special trigger circuit, as described previously, to place the record correctly on the oscillograph screen.

A uniform time delay between the detonation of the charge and the initiation of the sweep was attained in all cases by wrapping the charge with a few turns of a wire leading to the sweep-tripping circuit, and using the breaking of the wire to initiate the sweep-tripping impulse. If large currents are used the delay between the opening of the detonator bridge or heater wire, sometimes used to initiate the sweep, and the detonation, may be several milliseconds. Other investigators have noted this variation in the time of detonation (13) With the wire-wrapped charge, the time variation of the entire circuit from a set value was less than 20 microseconds.